Security Classification of This Report Has Been Cancelled

~~RESTRICTED~~ UNCLASSIFIED COPY NO. 6

RM No. E7L12

10 MAY 1948

RESEARCH MEMORANDUM

RELATION OF NOZZLE-BLADE AND TURBINE-BUCKET TEMPERATURES TO GAS TEMPERATURES IN A TURBOJET ENGINE

By J. Elmo Farmer

Flight Propulsion Research Laboratory
Cleveland, Ohio

CLASSIFICATION CANCELLED

CLASSIFIED DOCUMENT

This document contains classified information affecting the National Defense of the United States within the meaning of the Espionage Act, USC 50:31 and 32. Its transmission or the revelation of its contents in any manner to an unauthorized person is prohibited by law. Information so classified may be imparted only to persons in the military and naval services of the United States, appropriate civilian officers and employees of the Federal Government who have a legitimate interest therein, and to United States citizens of known loyalty and discretion who of necessity must be informed thereof.

Authority JW Crawley Date 12/4/53
EO 10501
By H-1-15-54 See above
R-72187

NATIONAL ADVISORY COMMITTEE FOR AERONAUTICS

WASHINGTON

April 30, 1948

NACA LIBRARY
LANGLEY MEMORIAL AERONAUTICAL LABORATORY
Langley Field, Va.

~~RESTRICTED~~ UNCLASSIFIED

Security Classification of This Report Has Been Cancelled

NASA Technical Library
3 1176 01425 9882

UNCLASSIFIED

NACA RM No. E7L12 RESTRICTED

NATIONAL ADVISORY COMMITTEE FOR AERONAUTICS

RESEARCH MEMORANDUM

RELATION OF NOZZLE-BLADE AND TURBINE-BUCKET TEMPERATURES TO GAS TEMPERATURES IN A TURBOJET ENGINE

By J. Elmo Farmer

SUMMARY

An investigation was conducted to determine experimentally turbine-nozzle-blade and turbine-bucket temperatures in a turbojet engine and to correlate these temperatures with the gas temperatures. Data were obtained over the normal range of engine speeds and with two tail-pipe-nozzle areas.

In general, the material temperature increased with increase in engine speed over the normal speed range of the engine. Maximum indicated temperatures were about 1900° F for the nozzle blade and 1500° F for the turbine bucket. Pronounced temperature gradients were found to exist along both the nozzle blade and the turbine bucket; these gradients varied both with rotor speed and with gas temperature. The maximum turbine-nozzle-blade temperature was 80° to 270° F higher than the calculated average turbine-inlet-gas temperature; the maximum turbine-bucket temperature was about 150° F less than the calculated average turbine-inlet-gas temperature. The maximum temperature reached by the turbine bucket during a normal engine start was lower than the temperature of the bucket during engine operation at maximum rated conditions.

INTRODUCTION

In order to evaluate properly the high-temperature alloys to be used in gas turbines, the temperature at which the materials will operate must be known. Data were therefore obtained at the NACA Cleveland laboratory to determine the temperature level and the temperature distribution in the turbine-nozzle blades and in the turbine buckets of a turbojet engine. These data also provide a basis for correlating turbine-bucket temperatures with gas temperatures; such a correlation will be helpful in predicting turbine-bucket operating temperatures in future engine designs.

RESTRICTED

UNCLASSIFIED

Security Classification of This Report Has Been Cancelled

Turbine-nozzle-blade and turbine-bucket temperatures were obtained for steady-state conditions over the normal range of engine operating speeds. The turbine-bucket and tail-pipe gas temperatures were also obtained during the interval in which the engine was being started.

The determination of turbine-bucket temperatures presents a difficult problem because of the high rotational speeds involved. A survey was made of the methods used by previous investigators to determine the temperatures of machine parts having high rotational speeds. The following methods were found to have been used with varying degrees of success:

1. Chemical paints that change color with temperature (references 1 and 2)

2. Fusible plugs that melt at different temperatures (reference 1)

3. Plugs of an age-hardenable steel, the hardening being a function of time and temperature (used by Army Air Forces)

4. Radiation pyrometers (references 1 and 3)

5. Electromotive force from thermocouples transmitted by induction (reference 4)

6. Electromotive force from thermocouples transmitted through chromel-alumel slip rings and brushes (reference 5)

7. Electromotive force from thermocouples transmitted through copper slip rings and brushes (reference 6)

The method of Fleissner and Viebmann (reference 6) was used to obtain these data. A thermocouple embedded in a material is a generally reliable means of measuring the temperature of the material. Copper brushes and slip rings were used because they generate no parasitic electromotive forces to interfere with the electromotive force generated by the thermocouple.

APPARATUS AND PROCEDURE

A turbojet engine having a dual-entry centrifugal compressor, a combustion-chamber assembly consisting of 14 individual burners, and a single-stage turbine having a rated speed of 11,500 rpm was used. The turbine disk was of an alloy having a nominal composition of 16 Cr, 25 Ni, 6 Mo, and 0.15 C, with the balance principally

Security Classification of This Report Has Been Cancelled

698

iron. The turbine-nozzle blades were AISI 347 stainless steel, and the turbine buckets were of an alloy of the following nominal composition: 62 Co, 28 Cr, 5.5 Mo, and 0.25 C. The engine was mounted on a sea-level pendulum-type test stand as shown in figure 1. It was operated on AN-F-32 fuel.

Turbine rotor speed was measured by a chronometric tachometer. Figure 2 shows the location of the thermocouples used to measure the tail-pipe gas temperature and the adjustable (variable-area) nozzle used to control the gas temperature. All of the tail-pipe gas temperatures were obtained by the 14 thermocouples at station 2 except for the data obtained during the starting interval at the beginning of run 2 when the four thermocouples at station 1 were used.

The turbine-inlet-gas total temperature had to be known to determine the relation of material temperature to gas temperature. Because gas-temperature data taken with thermocouples in the burner outlet are generally unreliable, the average turbine-inlet-gas total temperature was computed from the measured tail-pipe-gas temperature and the measured temperature rise across the compressor, as shown in appendix A.

Two runs were made with different locations of the thermocouples on the turbine-nozzle blades and the turbine buckets and with different tail-pipe-nozzle areas. Because of the type of tail-pipe nozzle used, the area of the nozzle was not determined. The following method of designating the nozzle areas will be used to simplify the discussion and the figures:

In run 1, the variable-area tail-pipe nozzle was adjusted to give an indicated gas total temperature in the tail pipe of 1145° F at a rotor speed of 11,500 rpm. This setting was held constant throughout run 1 and will hereinafter be designated the large tail-pipe nozzle.

In run 2, the variable-area tail-pipe nozzle was adjusted to give an indicated gas total temperature in the tail pipe of 1320° F at a rotor speed of 11,500 rpm. This nozzle setting was held constant throughout run 2 and will hereinafter be designated the small tail-pipe nozzle.

The maximum indicated tail-pipe-gas temperature allowed by the Army Air Forces during a ground check at 11,500 rpm is 1328° F (720° C).

Security Classification of This Report Has Been Cancelled

The locations of the thermocouples installed on the nozzle blade and on the turbine bucket for run 1 are shown in figure 3. In run 1, chromel-alumel thermocouples were spot-welded to the leading and trailing edges of the nozzle blade on the center line of the top burner. The thermocouples were located $2\frac{1}{2}$ inches above the base. Examination of previous nozzle-diaphragm failures showed that blades cracked more frequently at that location. The lead wires were shielded by a small tube and attached to the leading and trailing edges of the blade.

The location of the thermocouples installed on the nozzle blades and on the turbine bucket for run 2 is shown in figure 4(a). In run 2, four chromel-alumel thermocouples were embedded in the leading edge of each of three nozzle blades at the outlet of the top burner. The lead wires were brought out through drilled passages in the nozzle blades so that no protrusions disturbed the gas flow over the nozzle blades. The position of the instrumented nozzle blades with respect to the burner outlet is shown in figure 4(b). Chromel-alumel thermocouples were spot-welded to the convex side of the turbine bucket for both runs in the manner shown in figure 5.

During the starting interval at the beginning of run 2, a photographic record was made of the instruments indicating the rotor speed, the gas temperature at the exhaust-cone outlet (station 1, fig. 2), and the turbine-bucket temperature $2\frac{1}{4}$ inches above the root.

In order to install the thermocouple slip rings on a cool part of the engine, holes were drilled through the turbine wheel, the shaft, and the compressor rotor. These alterations allowed the slip rings to be installed on the accessory case, where they were cool and readily accessible.

The slip-ring assembly (fig. 6) consisted of 12 copper rings on a shaft driven by the engine at rotor speed. The brushes, also of copper, were so pivoted that a solenoid could pull them into contact with the slip rings. This arrangement decreased the brush wear as the brushes were kept in contact with the slip rings only while readings were being taken. The brush pressure during the contact period was adjusted to approximately 40 pounds per square inch. On the end of the assembly was a uniform-temperature box, which housed the junctions between the thermocouple lead wires and the copper wires that led to the slip rings, as indicated

Security Classification of This Report Has Been Cancelled

869

schematically in figure 7. Steam slightly above atmospheric pressure was supplied to the box to maintain the junctions at a uniform temperature. This arrangement allows remote operation of the brushes and transfers the effective cold junction to the potentiometer.

Before installation of the assembly on the engine, an investigation was conducted on a bench setup to determine the errors introduced by the slip rings. The errors were determined by impressing a voltage equivalent to that produced by a chromel-alumel thermocouple indicating a temperature of 2000° F on a circuit that was completed through the slip rings at several speeds within the range of engine operation. Comparison of the input and output voltages indicated a maximum error of 0.3 percent.

In run 1, data were obtained at rotor speeds of approximately 4000, 6000, 8000, 10,000, and 11,500 rpm. In the second run, turbine-bucket-temperature data were taken only at 10,000, 11,000, and 11,500 rpm in order to reduce over-all deterioration of the thermocouple installation.

RESULTS AND DISCUSSION

Basic data. - The basic data taken during the investigation are presented in figure 8 for the turbine-nozzle blades and in figure 9 for the turbine buckets. The calculated turbine-inlet-gas total temperature is plotted in both figures and the indicated tail-pipe-gas total temperature is shown in figure 9.

The data in figure 8(a) indicate that near the maximum rotor speed there is a temperature difference between the leading and trailing edges of the nozzle blade of about 40° F. Also, over the entire range of engine operation the material temperature near the middle of the blade is higher than the calculated turbine-inlet-gas total temperature, the difference being greater at the higher rotor speeds. In figure 8(b), the curves have been faired through data obtained at four points on the leading edge of the nozzle blade on the center line of the top burner. At maximum rotor speed (approximately 11,500 rpm), the data from the thermocouple located 1/2 and $1\frac{1}{2}$ inches above the base seemed to be incompatibly low, and so these points were disregarded in fairing in the curves. The nozzle blade reaches a maximum temperature of about 1900° F near the middle of the blade. Figure 8(c) presents the data from thermocouples in the leading edge $2\frac{1}{2}$ inches above the base of three nozzle blades at the outlet of burner 1. The blade in the center is at a higher temperature over the entire range of rotor speeds.

Security Classification of This Report Has Been Cancelled

869

The variation of the turbine-bucket temperature during run 1 over the normal range of rotor speeds is shown in figure 9(a). Also shown are the calculated turbine-inlet-gas total temperature and the indicated tail-pipe-gas total temperature.

Figure 9(b) presents similar data obtained in run 2. The data were obtained only at high rotor speeds. The turbine bucket reached a maximum temperature of about 1500° F near the middle of the bucket. The data for the point $3\frac{1}{4}$ inches above the base at a rotor speed of 10,000 rpm are apparently erroneous and cause the shape of that curve to be quite different from the others. The data presented in figure 9(a) are believed to be more nearly typical.

The general trend is for nozzle-blade and turbine-bucket temperatures to increase with rotor speed over the normal speed range. An exception to this generalization of variation in temperature with change in engine speed occurs at low speeds at which the enriched fuel-air ratio increases the gas temperature. This enrichment causes the material temperatures to be as high at 4000 as at 10,000 rpm (except for fig. 8(a)).

Turbine-nozzle-blade temperature distribution. - The temperature distribution existing in the turbine-nozzle blades is shown in figure 10 as a function of thermocouple location and rotor speed. This figure is a cross plot of data from figure 8(b). These curves show that the temperature gradient along the blade is a smooth curve and that the magnitude of the gradient increases with increasing gas temperature as the rotor speed is increased. A maximum indicated temperature of about 1930° F is reached at 11,500 rpm in about the center of the blade. At the same engine conditions the temperature at the tip of the blade is about 1380° F; the average temperature gradient between the center and the tip is about 220° F per inch. The peak temperature is shifted towards the base of the blade as rotor speed is increased and the difference between blade-base temperature and blade-tip temperature increased considerably as rotor speed is increased. The shift in the temperature peak may be due to the angle at which the burner is set with respect to the nozzle blades and to the asymmetrical shape of the burner outlet.

The nozzle-blade temperature as a function of the blade position with respect to the burner outlet is shown in figure 11. This figure is a cross plot of the data from figure 8(c). The data are from thermocouples in the leading edge $2\frac{1}{2}$ inches above the blade base. The temperature distribution indicates that the maximum gas temperatures are near the center of the burner outlet, as would be expected from the design of the burner.

Security Classification of This Report Has Been Cancelled

Turbine-bucket-temperature distribution. - The temperature distribution radially along the turbine bucket as a function of rotor speed is shown in figure 12, which is a cross plot of data from figure 9.

The method of attaching the thermocouple junctions to the turbine bucket may have disturbed the gas flow sufficiently to alter the temperature of the bucket. At present, no means are available for evaluating the effect of the disturbance in gas flow on the temperature of the material.

The indicated temperature distribution along the turbine bucket is similar to that of the turbine-nozzle blade. A change in the temperature level of the engine affects both the magnitude of the temperature gradients and the magnitude of the peak temperature. The same shift in the peak temperature and increase in blade-base temperature can be seen as in the nozzle blade and is probably due to the position and shape of the burner outlet. The 10,000-rpm curve in figure 12(b) is dotted over the outer half of the bucket because the datum point shown in figure 9(b) is believed to be in error.

Temperature distribution of gas at burner-outlet. - The results of a gas-temperature survey made at the outlet of the top burner are given in figure 13. The data plotted are indicated temperatures obtained with three bare chromel-alumel thermocouple probes. All three of the probes could not be operated simultaneously; therefore a survey was made with each probe while the engine operating conditions were held as constant as possible. The location of the probes was not entirely satisfactory, and the bare thermocouples are undoubtedly subject to radiation errors. The figure does, however, show that the hottest gas is at the center of the burner. The highest temperature measured was 2175° F at a speed of 11,500 rpm (fig. 13(c)). The temperatures at the top of the burner are generally lower than at the bottom. This fact may account for the low material temperatures at the tip of the nozzle blades and the turbine buckets. The temperature distribution in nozzle blades and turbine buckets is probably the result of the temperature gradient in the gas issuing from the burner plus some cooling due to the heat transfer through the blade base and the bucket roots.

Turbine-bucket temperatures during starting. - Figure 14 shows the relation between engine speed and indicated tail-pipe-gas total temperatures during a typical starting operation (run 2). The exact shapes of curves such as these are dependent upon the manipulation of the throttle during the starting period.

Security Classification of This Report Has Been Cancelled

The maximum indicated tail-pipe-gas total temperature at the exhaust-cone outlet (station 1, fig. 2) is 1500° F. The turbine-bucket temperature lags a little behind the gas temperature and reaches a maximum of 1370° F about 7 seconds after the gas temperature reached a peak. During this start, the temperature of the turbine-bucket material increased from 200° to 1370° F in 27 seconds, or at the rate of 43° F per second. These conditions are quite severe and indicate that any materials that are to be used in gas turbines will need high resistance to thermal shock. These data indicate that during a normal engine start the maximum temperature reached by the turbine bucket is about 100° F less than when the bucket is operating at maximum rated engine conditions.

Relation of material and gas temperatures. - The nozzle-blade temperature is plotted as a function of the calculated turbine-inlet-gas total temperature in figure 15. The curves were determined by using a method of least squares. The curves have slopes varying from 0.90 for the point $2\frac{1}{2}$ inches above the base to 1.32 for the point 1/2 inch above the base. The differences between individual curves are caused by temperature gradients existing along a given blade or from blade to blade. The maximum nozzle-blade temperature is from 80° to 270° F higher than the calculated average turbine-inlet-gas total temperature.

Similar data for the turbine bucket (fig. 16) show that the turbine-bucket temperature is in all cases below the turbine-inlet-gas total temperature and that the differences between the various bucket temperatures and the gas temperature are nearly constant with changing gas temperature. The slope of the curves vary from about 0.92 to 0.97. The curve was not drawn through the data from $3\frac{1}{4}$ inches above the base because the data was in error, as previously explained. The maximum turbine-bucket temperature is about 150° F less than the calculated turbine-inlet-gas total temperature.

SUMMARY OF RESULTS

An investigation of the material temperatures in the nozzle blades and the turbine buckets of a turbojet engine gave the following results:

1. The material temperatures increased, in general, with increase in rotor speed within the normal speed range of the engine. Maximum indicated temperatures were about 1900° F for the nozzle blade and 1500° F for the turbine bucket.

Security Classification of This Report Has Been Cancelled

2. Pronounced temperature gradients existed in both the nozzle blade and the turbine bucket. These gradients varied with rotor speed and with gas temperature.

3. Nozzle-blade temperatures were generally higher than the calculated turbine-inlet-gas total temperature. The maximum nozzle-blade temperature was 80° to 270° F higher than the calculated turbine-inlet-gas total temperature. The turbine-bucket temperatures were well below the calculated turbine-inlet-gas total temperature. The maximum turbine-bucket temperature was about 150° F less than the calculated turbine-inlet-gas total temperature.

4. During the starting interval of the engine, the turbine-bucket temperature followed the tail-pipe gas temperature closely, with some time lag in evidence. The maximum turbine-bucket temperature during a normal engine start was about 100° F lower than that when the engine was operated at maximum rated engine conditions.

Flight Propulsion Research Laboratory,
National Advisory Committee for Aeronautics,
Cleveland, Ohio.

Security Classification of This Report Has Been Cancelled

APPENDIX A - CALCULATION OF TURBINE-INLET-GAS TOTAL TEMPERATURE

Symbols

The following symbols are used in the calculation:

$c_{p,c}$ specific heat at constant pressure in compressor, Btu/(lb)(°F)

$c_{p,t}$ specific heat at constant pressure in turbine, Btu/(lb)(°F)

hp_c compressor horsepower

hp_t turbine power

P total pressure, lb/sq ft absolute

p static pressure, lb/sq ft absolute

T_3 turbine-inlet-gas total temperature, °R

T_4 tail-pipe-gas total temperature, °R

$T_{i,4}$ indicated tail-pipe gas temperature, °R

t_4 tail-pipe-gas static temperature, °R

ΔT_c compressor temperature rise, °F

ΔT_t turbine temperature drop, °F

W_a air flow, lb/sec

W_g gas flow, lb/sec

γ ratio of specific heats of gases

Method of Calculation

Unpublished data obtained at the NACA Cleveland laboratory on a cold calibration of a sample thermocouple of the type used at air speeds up to a Mach number of about 0.8 showed that the thermocouple measured the static temperature plus approximately 76 percent of the adiabatic temperature rise caused by the impact of the air on the thermocouple. Static temperature t_4 was determined by application of this factor to observed values of temperature and pressure in the following manner:

Security Classification of This Report Has Been Cancelled

869

$$t_4 = \frac{T_{i,4}}{1 + 0.76\left[\left(\frac{P}{p}\right)^{\frac{\gamma-1}{\gamma}} - 1\right]}$$

The total temperature T_4 was determined from

$$T_4 = t_4\left(\frac{P}{p}\right)^{\frac{\gamma-1}{\gamma}} = \frac{T_{i,4}\left(\frac{P}{p}\right)^{\frac{\gamma-1}{\gamma}}}{1 + 0.76\left[\left(\frac{P}{p}\right)^{\frac{\gamma-1}{\gamma}} - 1\right]}$$

It was assumed that the power developed by the turbine was equal to that required by the compressor:

$$hp_c = \frac{778}{550} c_{p,c}\Delta T_c W_a = hp_t = \frac{778}{550} c_{p,t}\Delta T_t W_g$$

and that the weight of hot gas through the turbine was equal to the weight of air through the compressor:

$$c_{p,c}\Delta T_c = c_{p,t}\Delta T_t$$

Therefore

$$\Delta T_t = \Delta T_c \frac{c_{p,c}}{c_{p,t}}$$

The turbine-inlet-gas total temperature T_3 is the sum of the tailpipe-gas total temperature and the temperature drop in the turbine:

$$T_3 = T_4 + \Delta T_t$$

Security Classification of This Report Has Been Cancelled

REFERENCES

1. Leist, K., and Knörnschild, E.: Temperature Measurements of High-Speed Machine Parts. British R. T. P. Trans. No. 2205, Ministry Aircraft Prod. (From Jahrb. Luftfahrtforschung, vol. 2, 1937, pp. 289-294.)

2. Fenzig, F.: Temperature-Indicating Paints. NACA TM No. 905, 1939.

3. Head, Victor P.: Radiation Pyrometry in Turbosupercharger Testing. Instr., vol. 17, no. 1, Jan. 1944, pp. 36-40.

4. Gnam, E.: A New Apparatus for Measuring the Temperature at Machine Parts Rotating at High Speeds. NACA TM No. 1080, 1945.

5. Hartwig, Frederick, J., Jr.: Comparative Effectiveness of a Convection-Type and a Radiation-Type Cooling Cap on a Turbosupercharger. NACA TN No. 1082, 1946.

6. Fleissner, G., and Viebmann, H.: Method for Measurement of Very Small Electromotive (Thermo) Forces through Slip Rings. Trans. No. F-TS-483-RE, Air Materiel Command, Army Air Forces, Oct. 1946. (Abs. in Bib. Sci. and Ind. Res., vol. 2, no. 4, 1946, p. 266, PB22307.)

669

Security Classification of This Report Has Been Cancelled

869

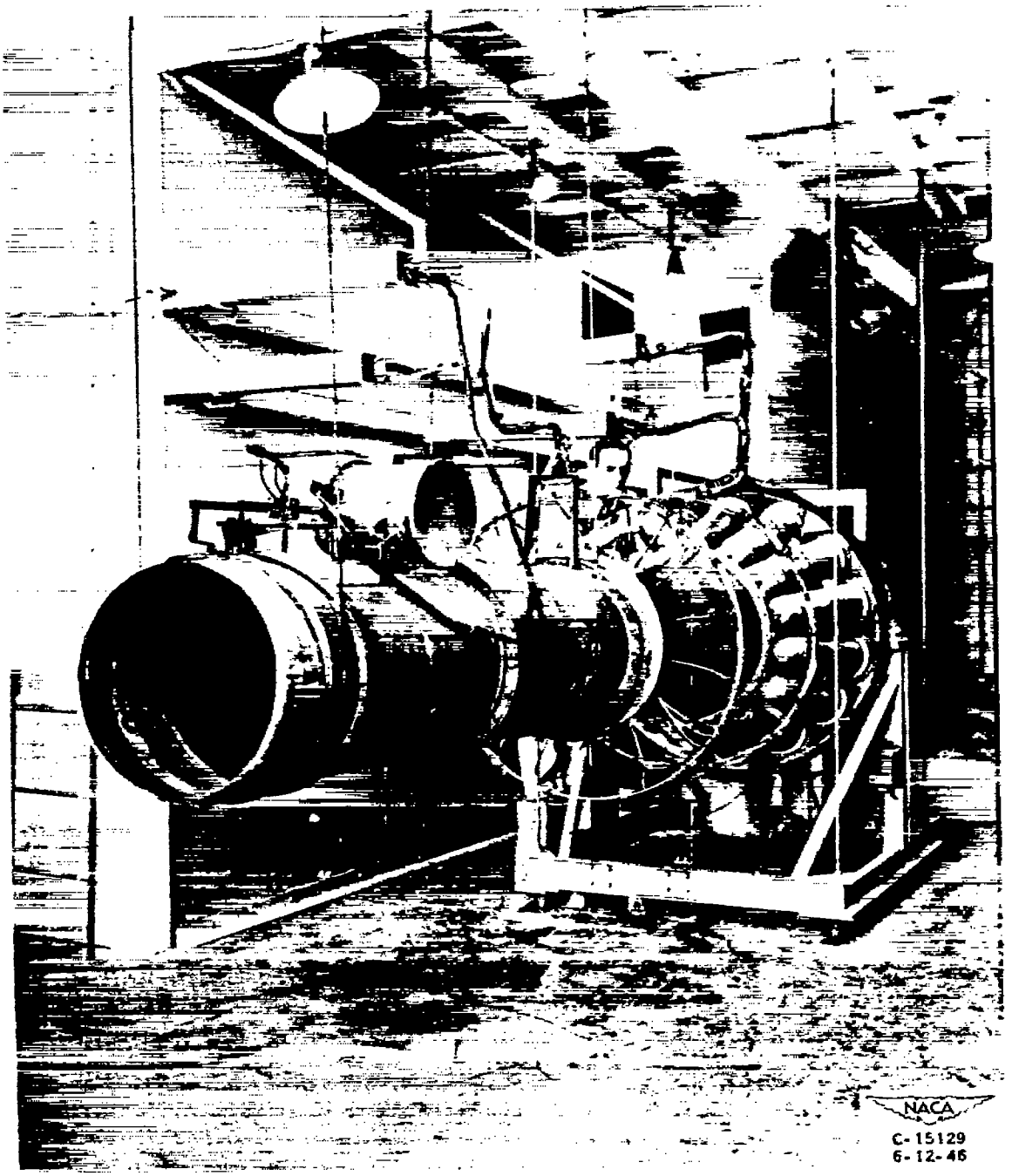

Figure 1. – Turbojet engine mounted on sea-level pendulum-type test stand.

Security Classification of This Report Has Been Cancelled

Security Classification of This Report Has Been Cancelled

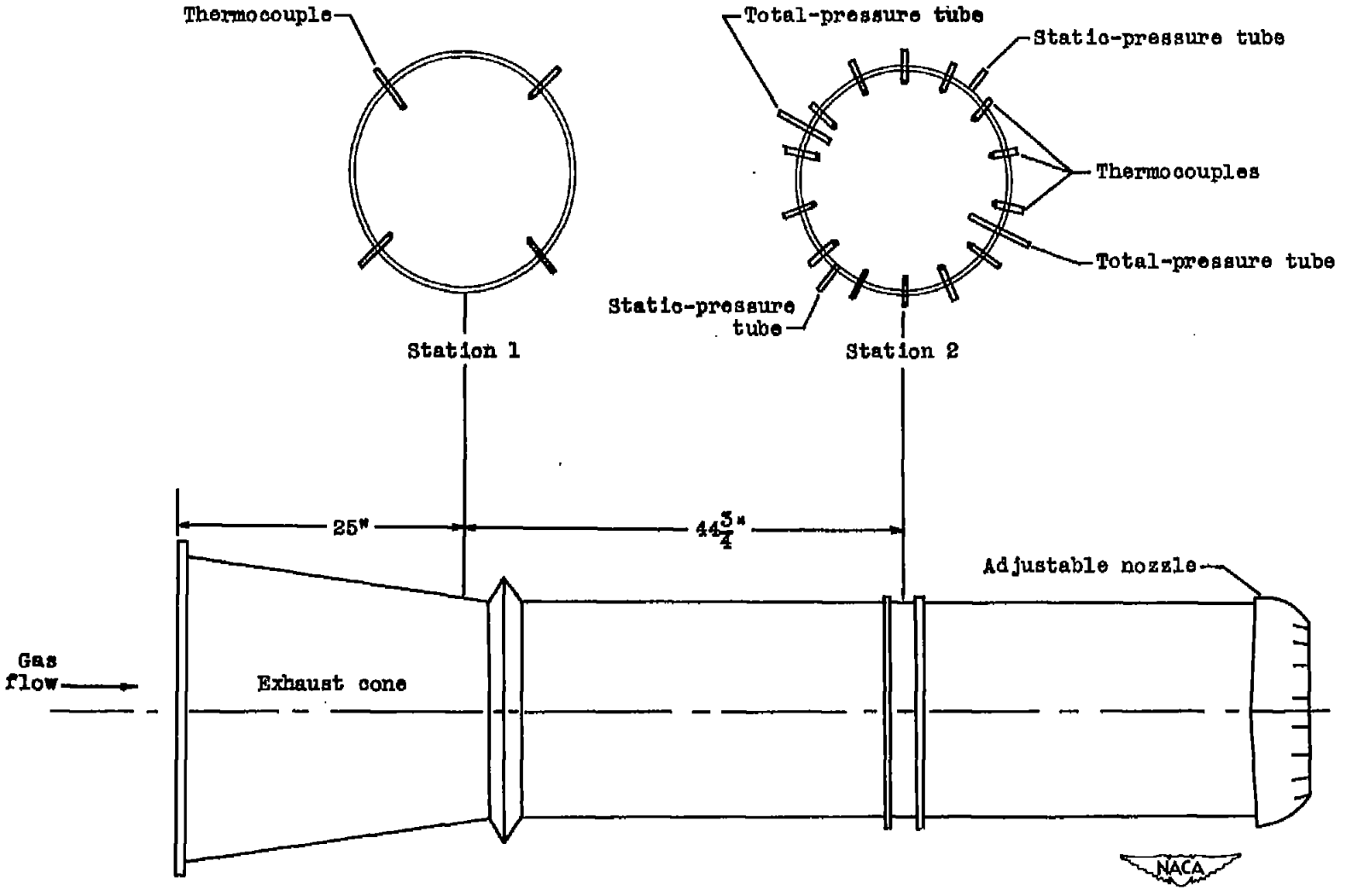

Figure 2. - Location of tail-pipe instrumentation.

Security Classification of This Report Has Been Cancelled

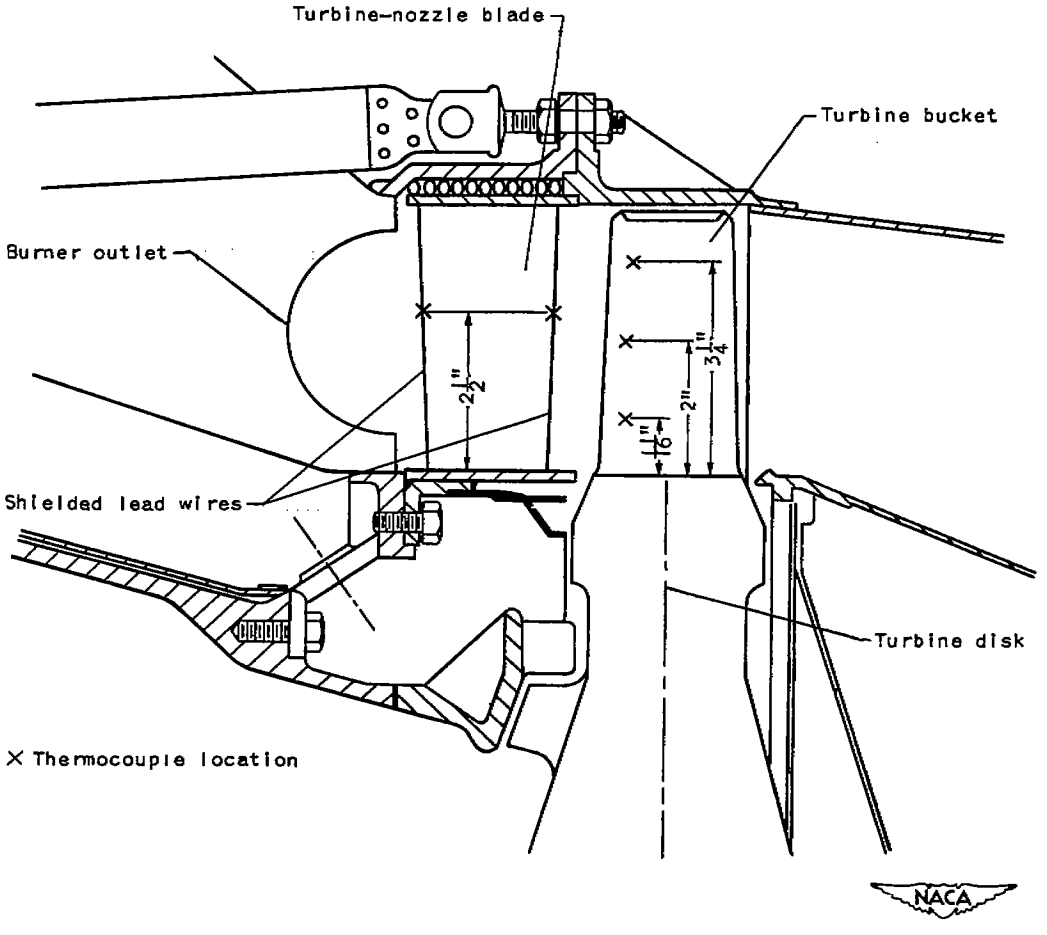

Figure 3. – Location of thermocouples on leading and trailing edges of turbine-nozzle blade (on center line of top burner) and on convex side of turbine bucket during run 1.

869

120-1094

Security Classification of This Report Has Been Cancelled

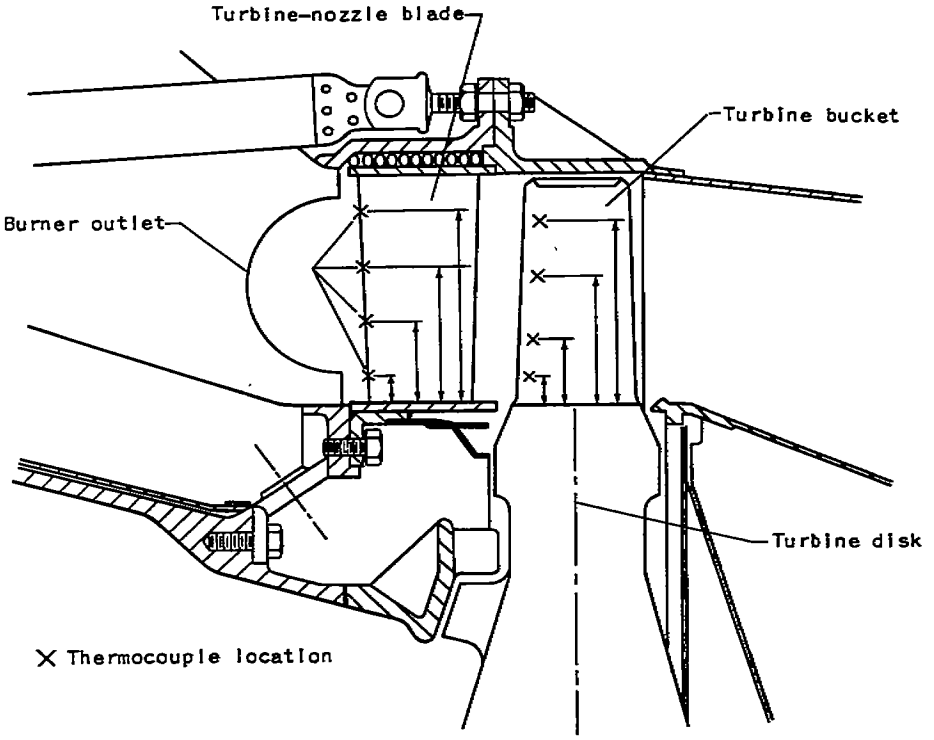

(a) Thermocouple locations.

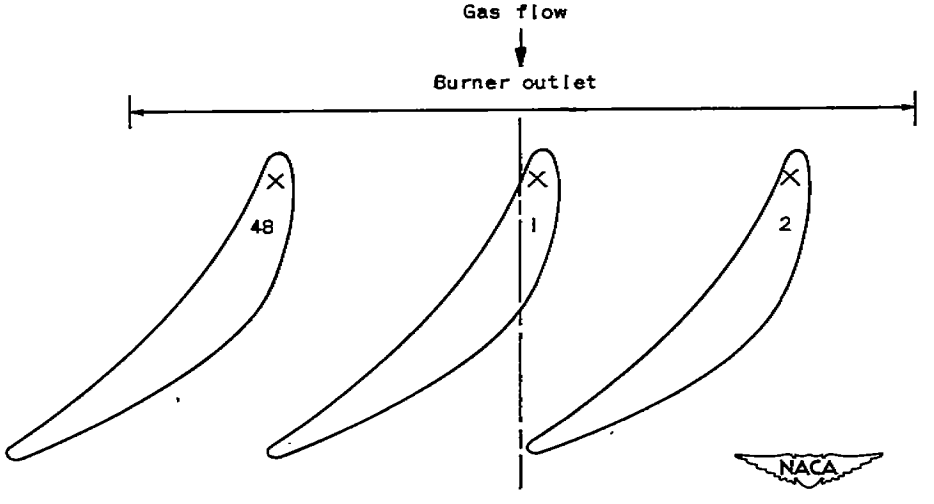

(b) Position of turbine-nozzle blades behind top burner.

Figure 4. - Location of the thermocouples on leading edge of turbine-nozzle blades and on convex side of turbine bucket during run 2.

Security Classification of This Report Has Been Cancelled

Security Classification of This Report Has Been Cancelled

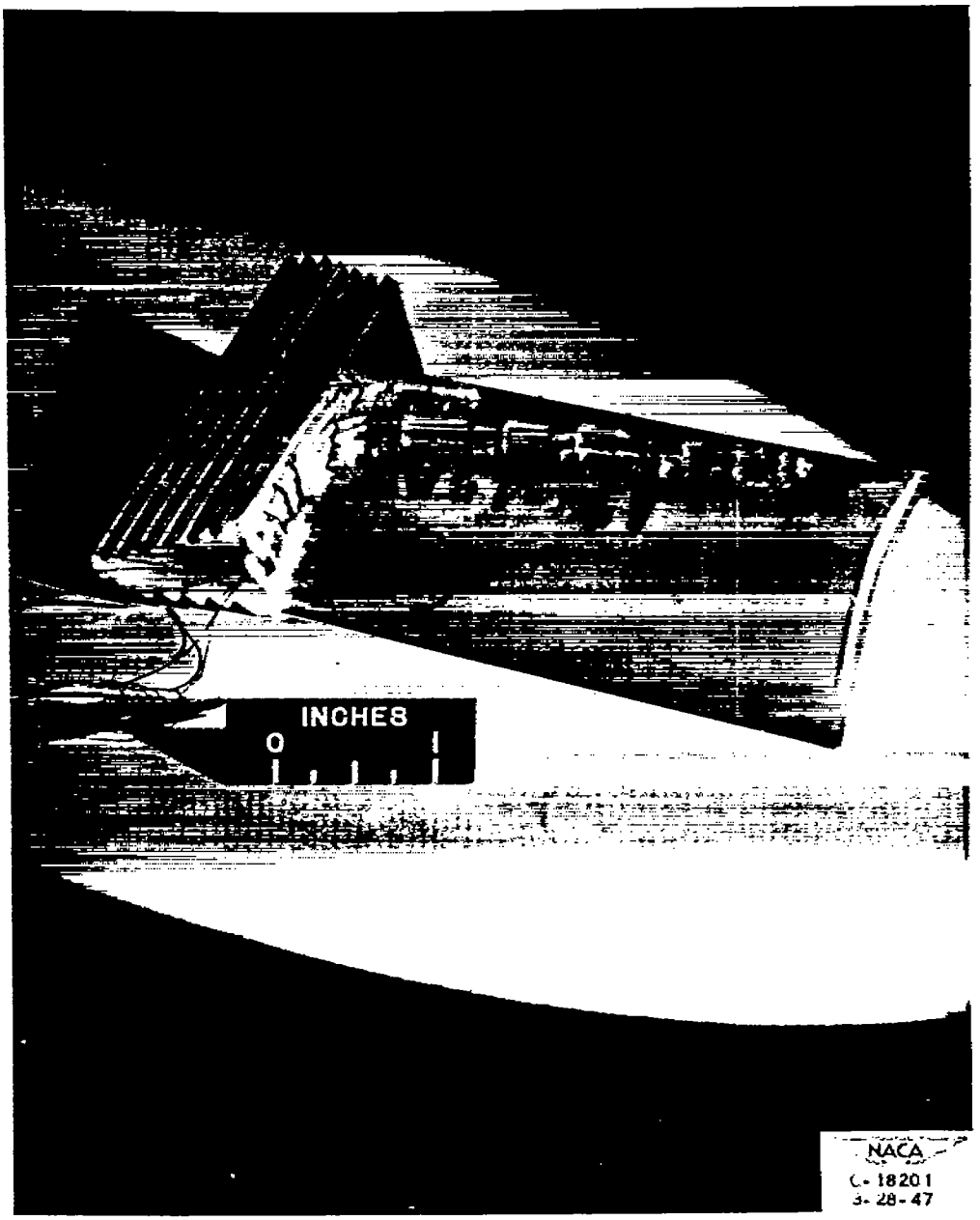

Figure 5. – Thermocouples installed on convex side of turbine bucket.

Security Classification of This Report Has Been Cancelled

Security Classification of This Report Has Been Cancelled

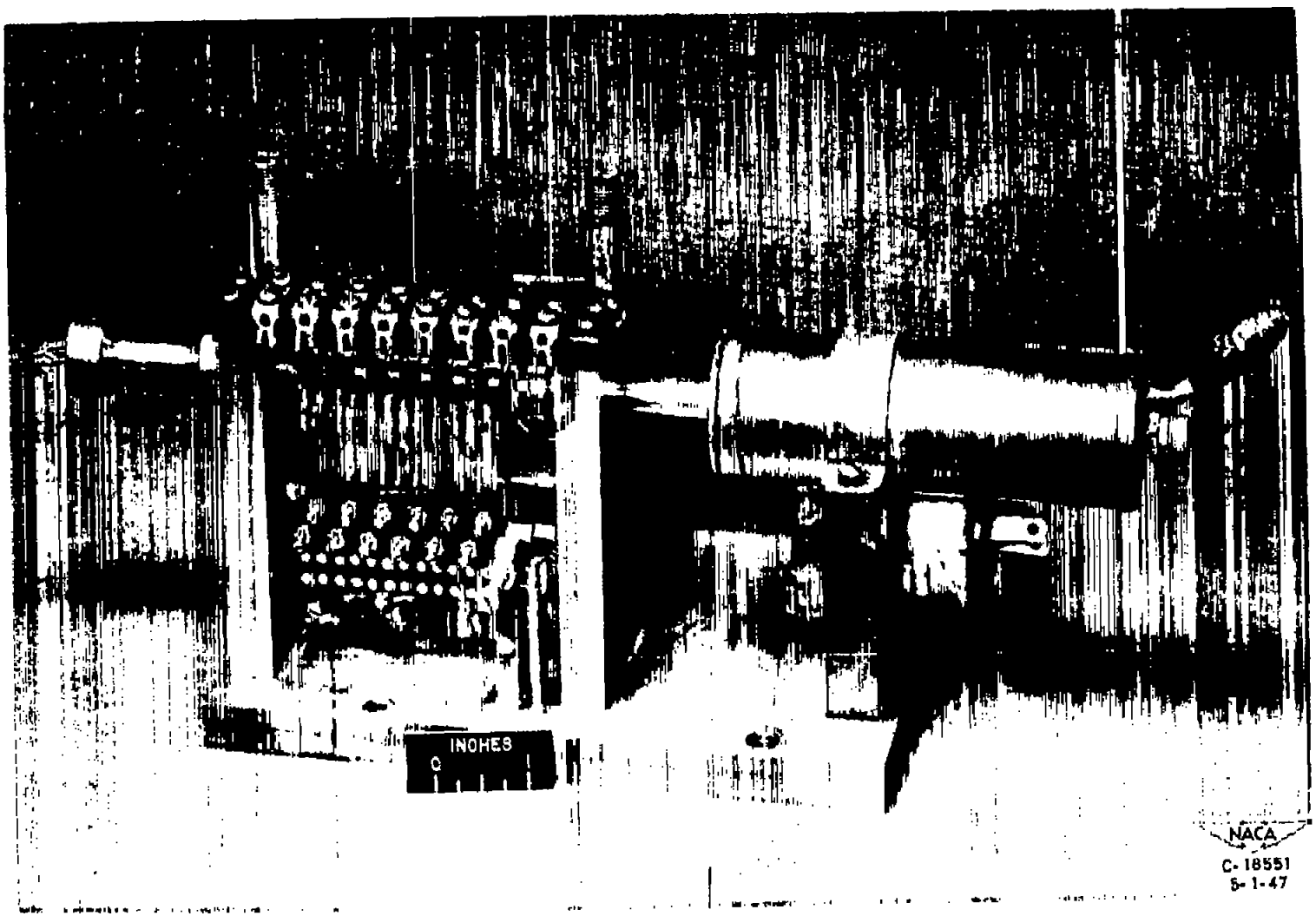

Figure 6. - Thermocouple slip-ring assembly used in measuring turbine-bucket temperatures.

Security Classification of This Report Has Been Cancelled

Security Classification of This Report Has Been Cancelled

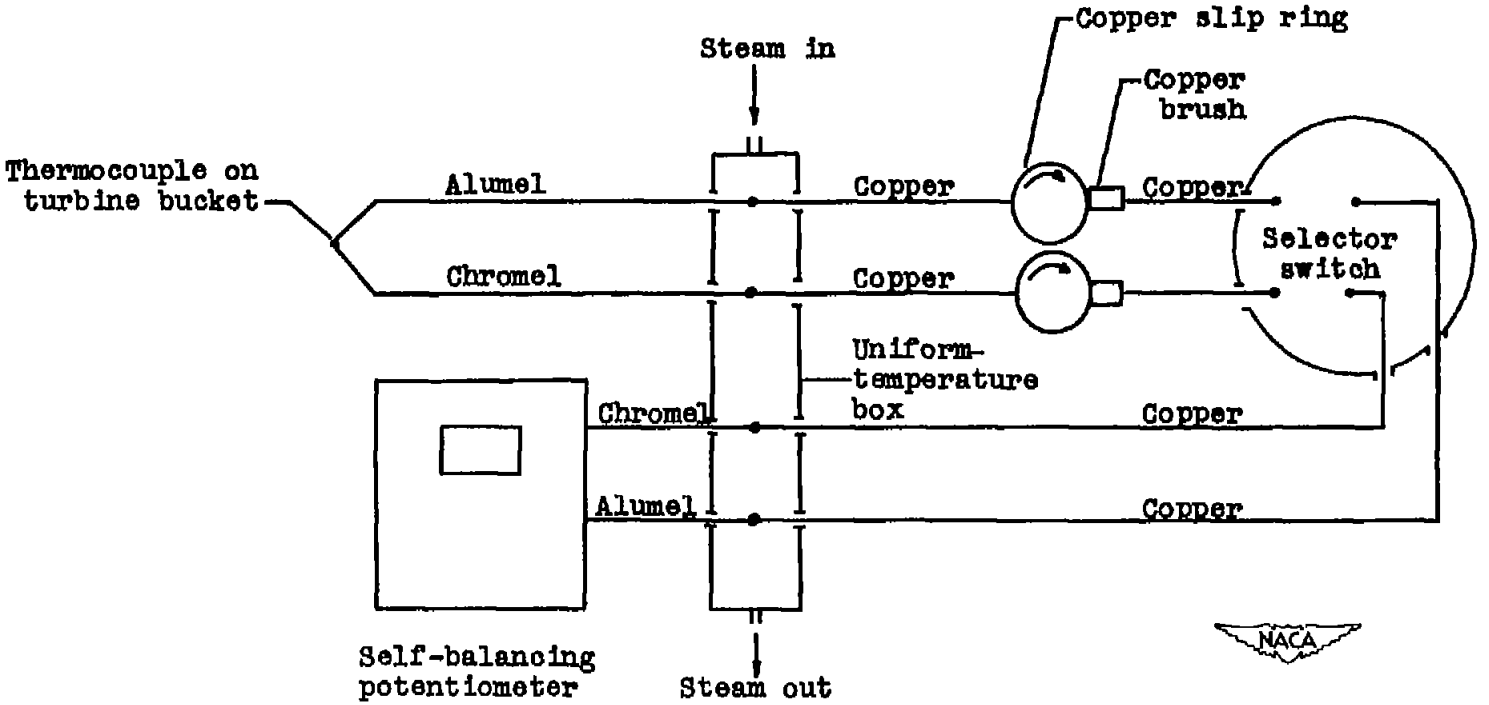

Figure 7. - Schematic diagram of thermocouple installation for measuring turbine-bucket temperatures.

Security Classification of This Report Has Been Cancelled

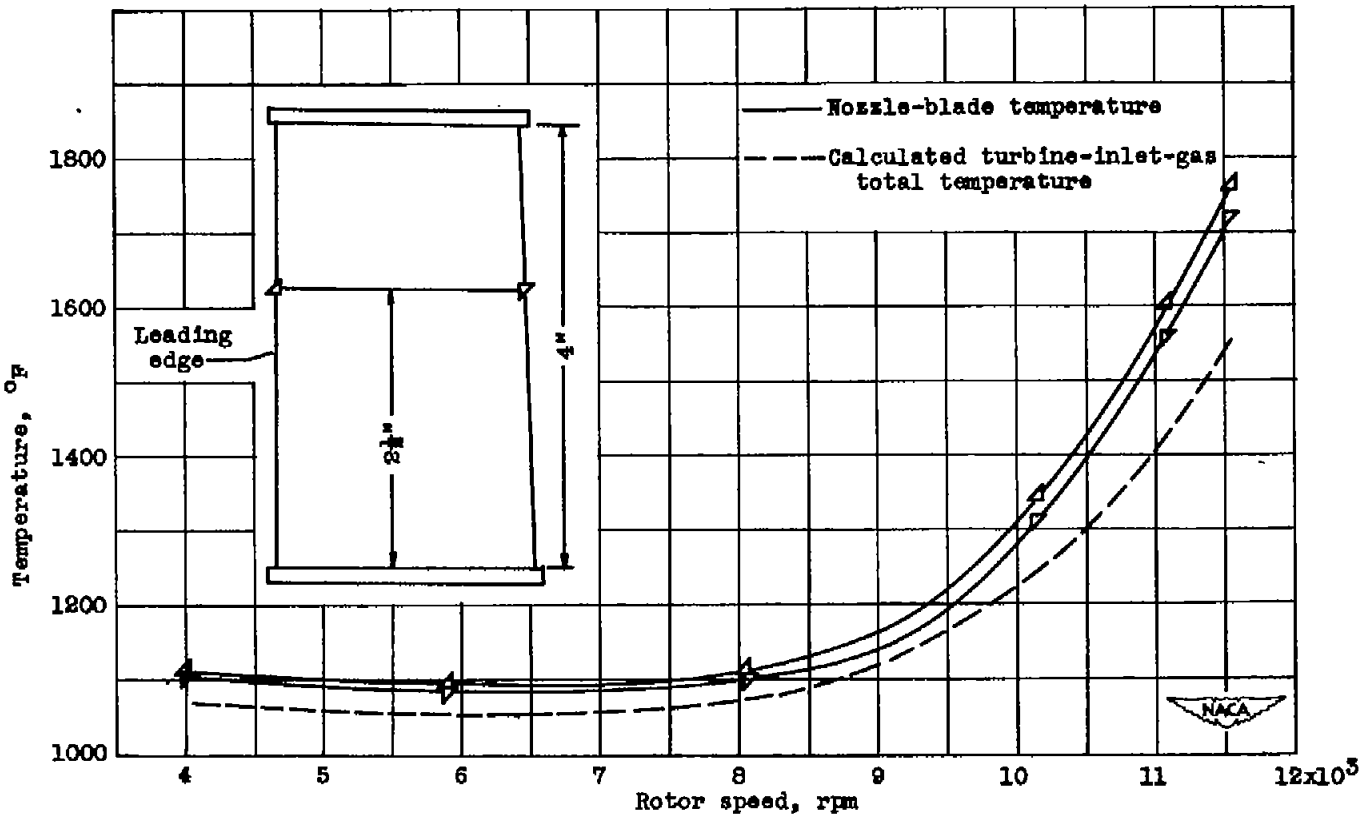

(a) Run 1 (large tail-pipe nozzle); thermocouples on leading and trailing edge on nozzle blade 1.

Figure 8. - Variation of turbine-nozzle-blade temperature with rotor speed in turbojet engine at sea level.

Security Classification of This Report Has Been Cancelled

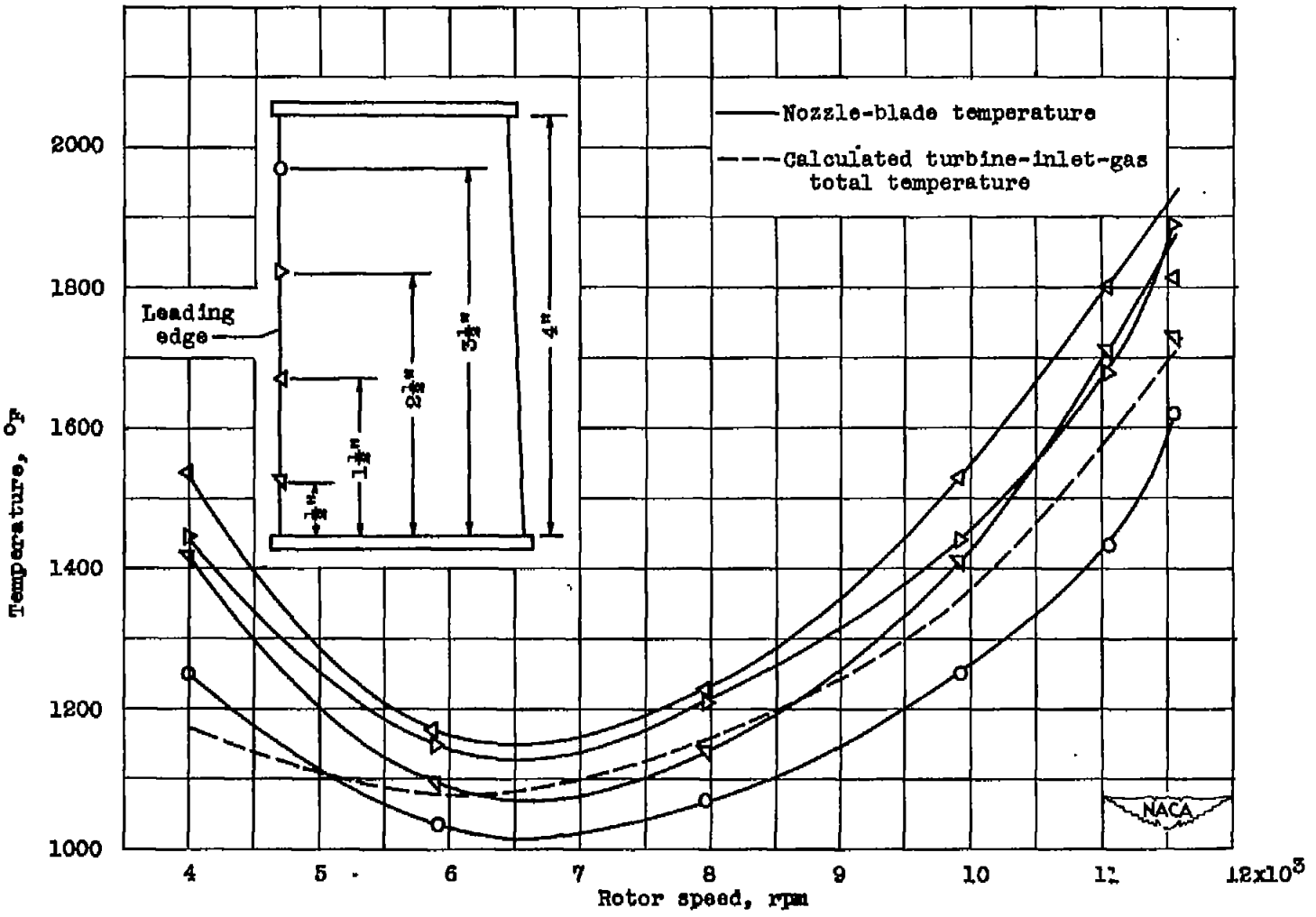

(b) Run 2 (small tail-pipe nozzle); four thermocouples on leading edge of nozzle-blade 1.

Figure 8. - Continued. Variation of turbine-nozzle-blade temperature with rotor speed in turbojet engine at sea level.

Security Classification of This Report Has Been Cancelled

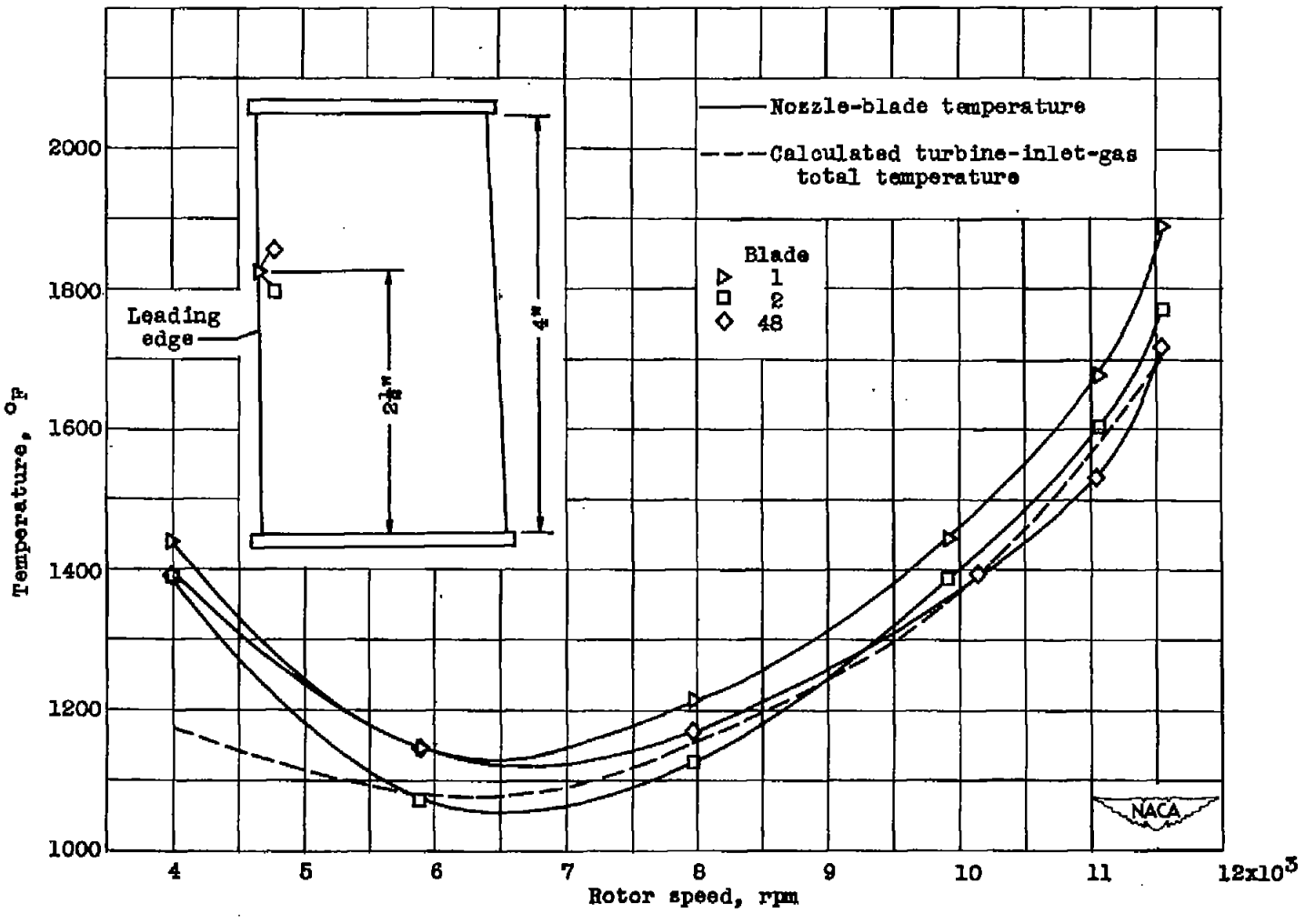

(c) Run 2 (small tail-pipe nozzle); thermocouples on leading edge of three blades at outlet of top burner.

Figure 8. - Concluded. Variation of turbine-nozzle-blade temperature with rotor speed in turbojet engine at sea level.

Security Classification of This Report Has Been Cancelled

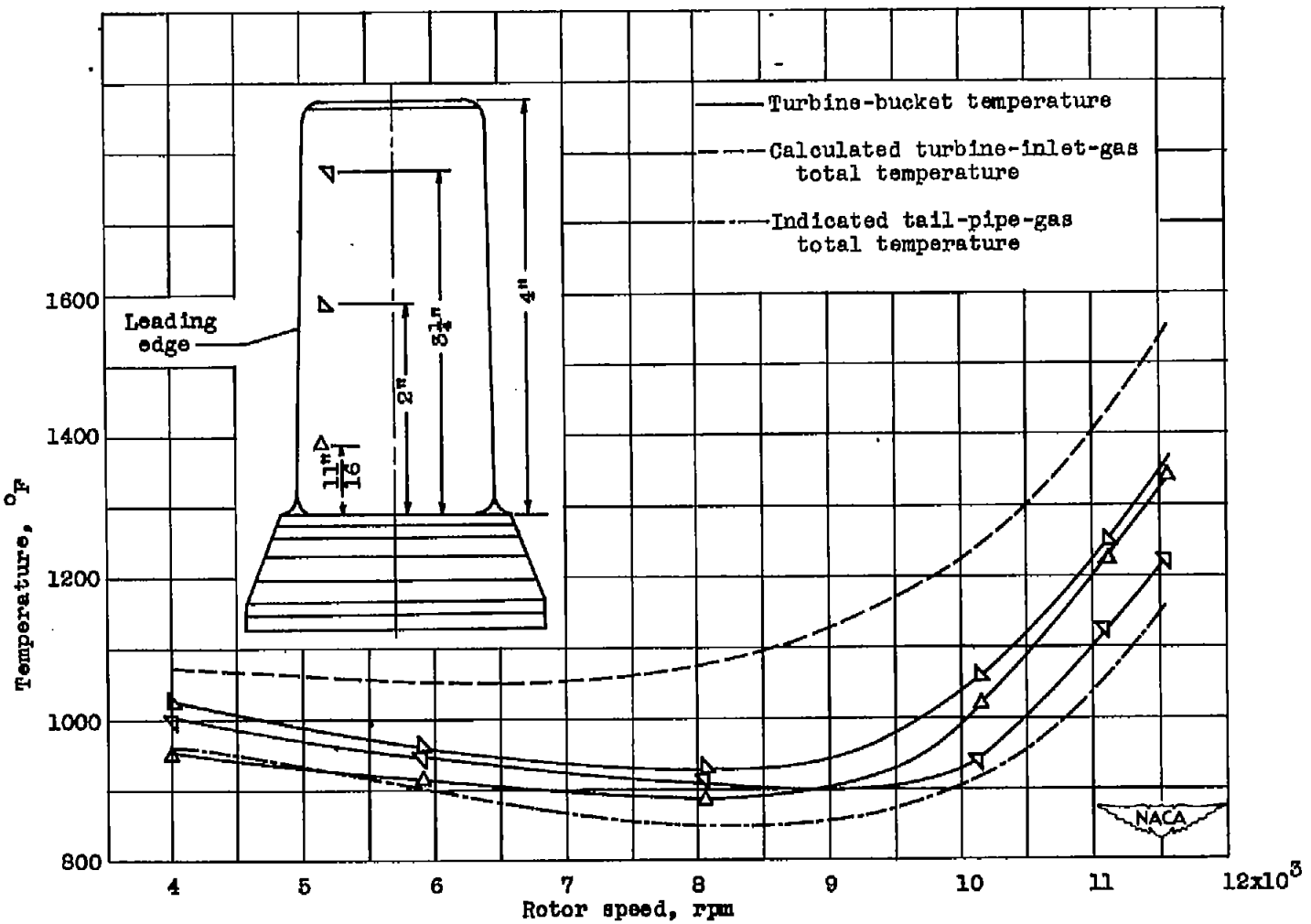

(a) Run 1 (large tail-pipe nozzle).

Figure 9. - Variation of turbine-bucket temperature with rotor speed in turbojet engine at sea level.

Security Classification of This Report Has Been Cancelled

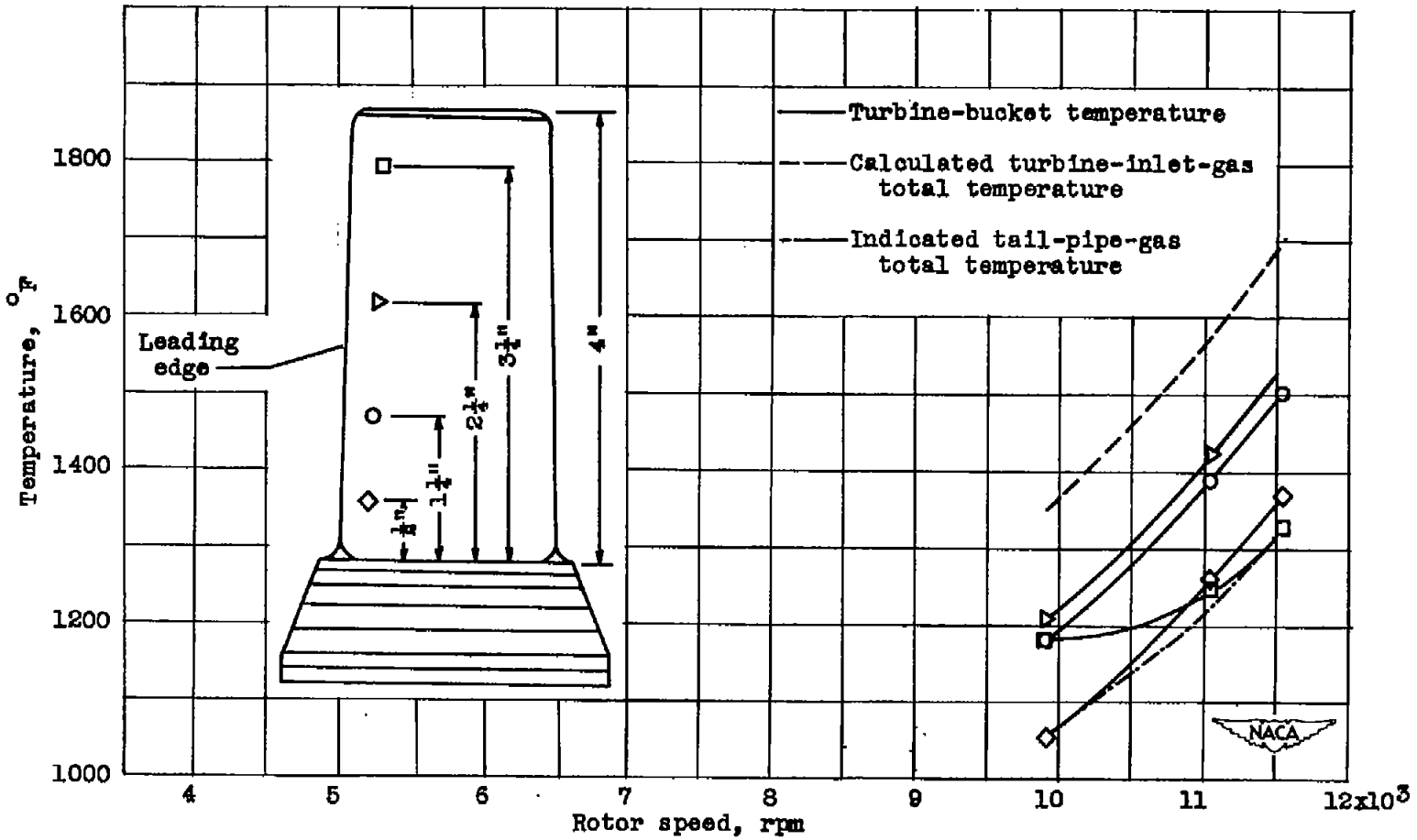

(b) Run 2 (small tail-pipe nozzle).

Figure 9. - Concluded. Variation of turbine-bucket temperature with rotor speed in turbojet engine at sea level.

Security Classification of This Report Has Been Cancelled

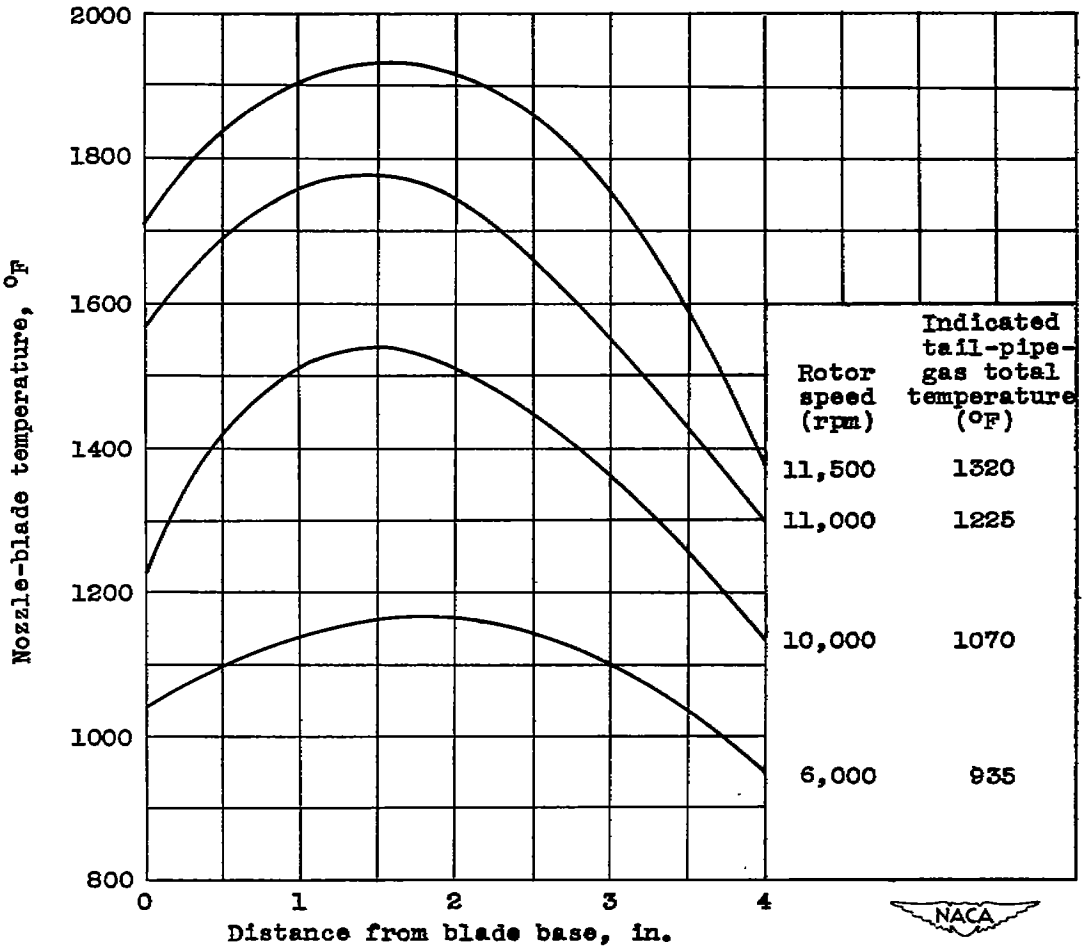

Figure 10. - Temperature distribution along turbine-nozzle blade 1 in turbojet engine at several engine speeds for run 2 (small tail-pipe nozzle). (Cross plot of data from fig. 8(b).)

Security Classification of This Report Has Been Cancelled

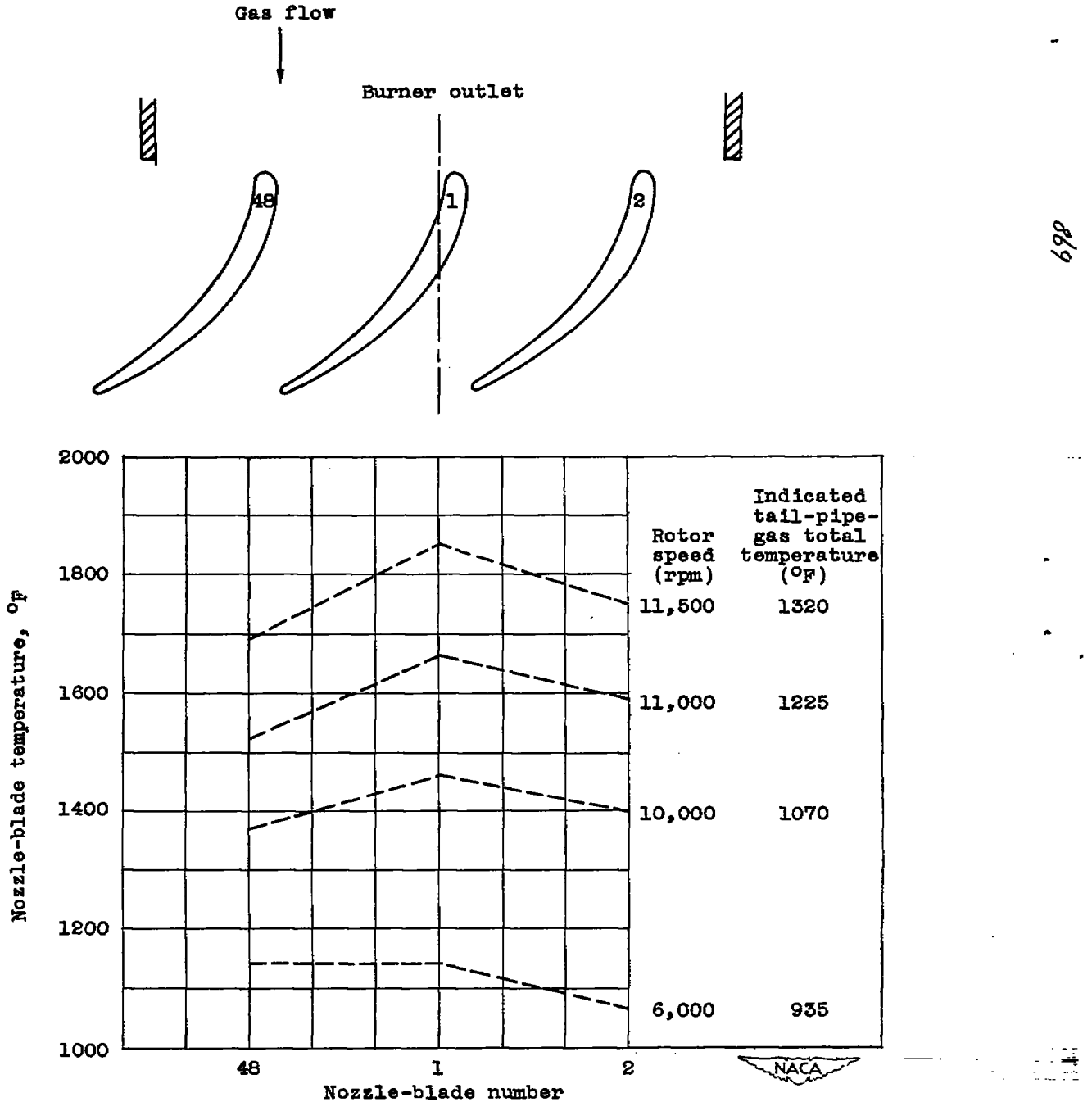

Figure 11. - Nozzle-blade temperature with respect to burner outlet in turbojet engine for run 2 (small tail-pipe nozzle). Data from thermocouples in leading edge $2\frac{1}{2}$ inches above blade base. (Cross plot of data from fig. 8(c).)

Security Classification of This Report Has Been Cancelled

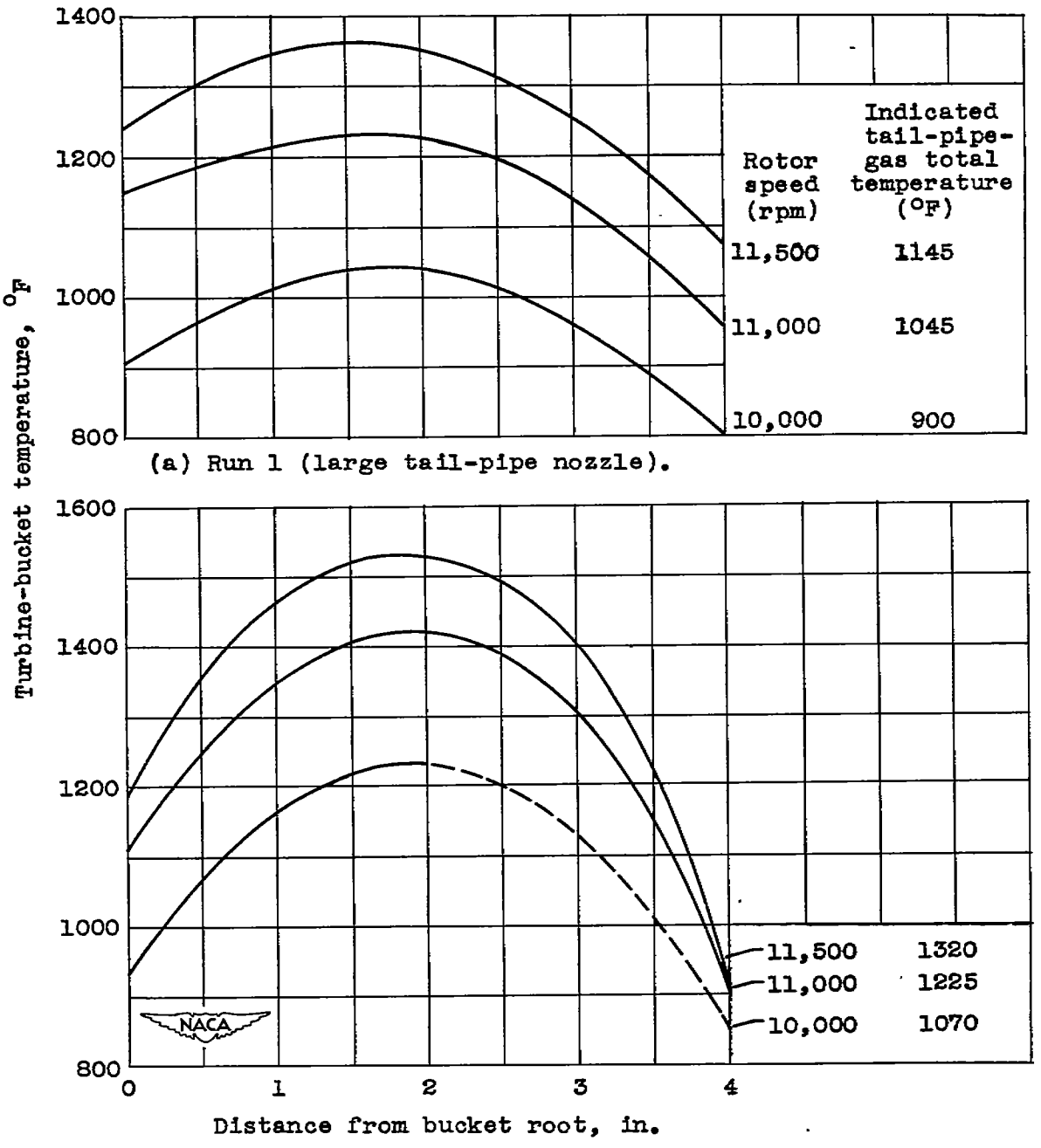

(a) Run 1 (large tail-pipe nozzle).

(b) Run 2 (small tail-pipe nozzle).

Figure 12. - Temperature gradients along turbine bucket in turbojet engine. (Cross plot of data from fig. 9.)

Security Classification of This Report Has Been Cancelled

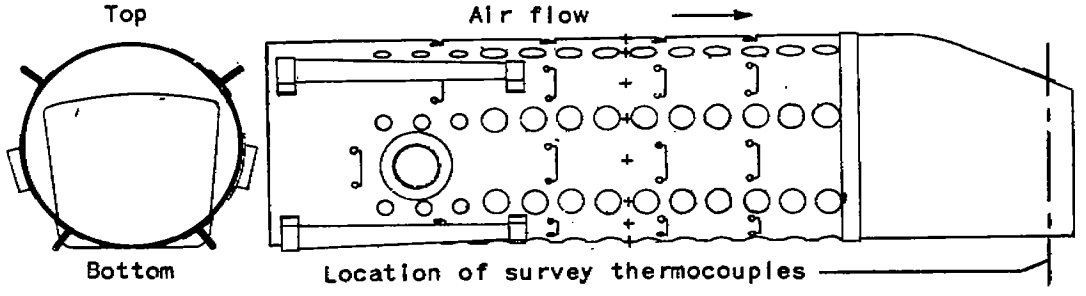

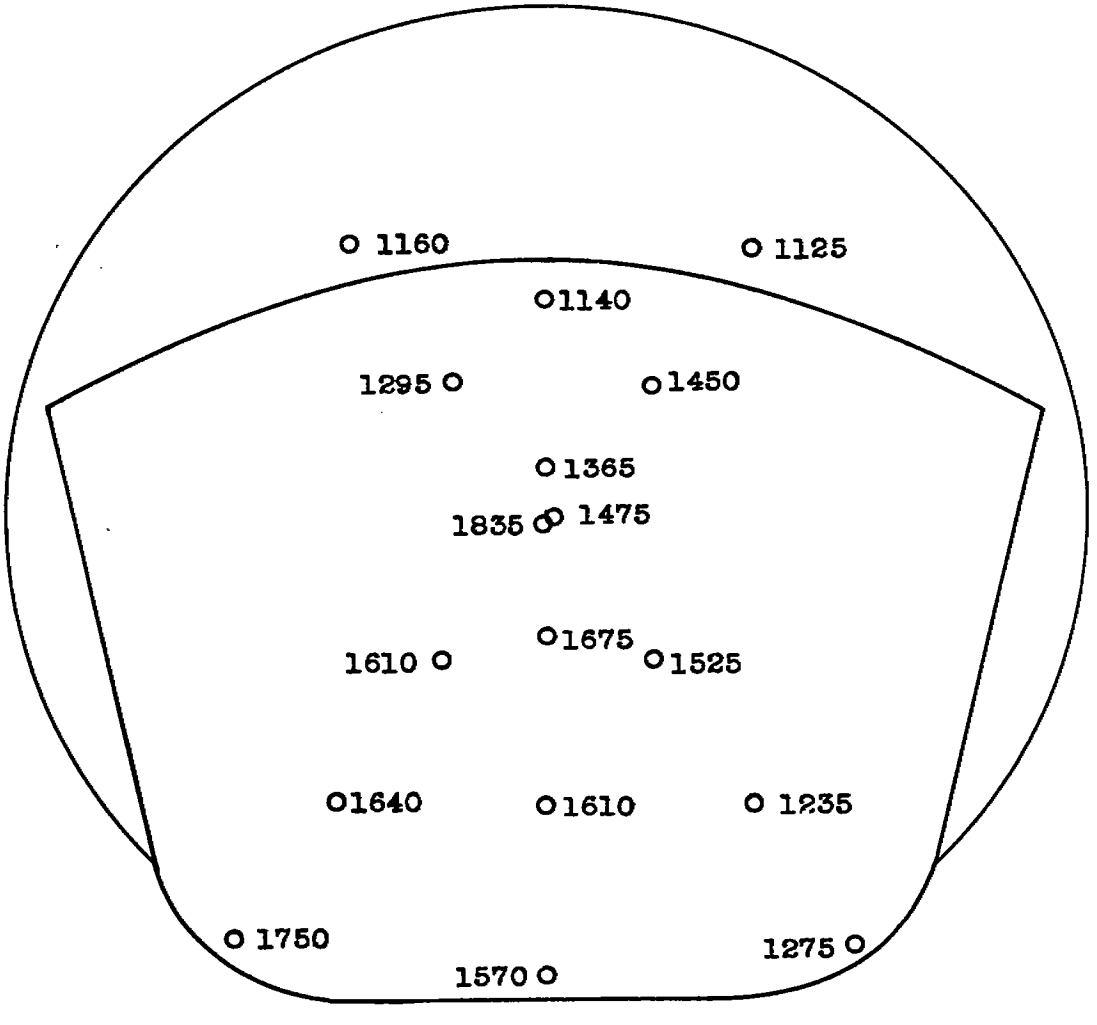

(a) Rotor speed, about 10,000 rpm.

Figure 13. - Temperature distribution in gas issuing from burner.

Security Classification of This Report Has Been Cancelled

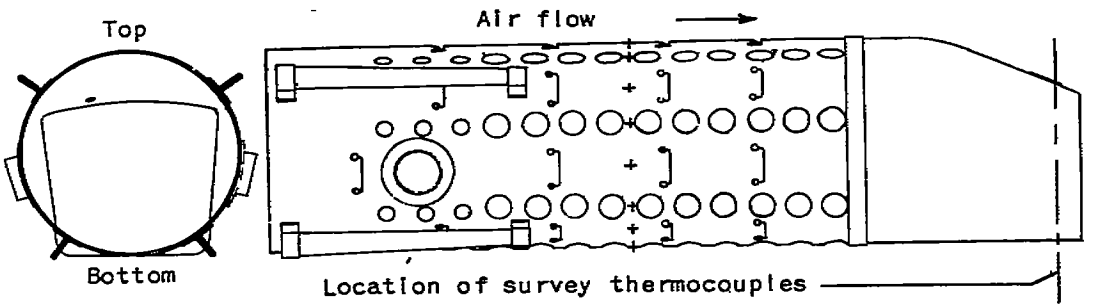

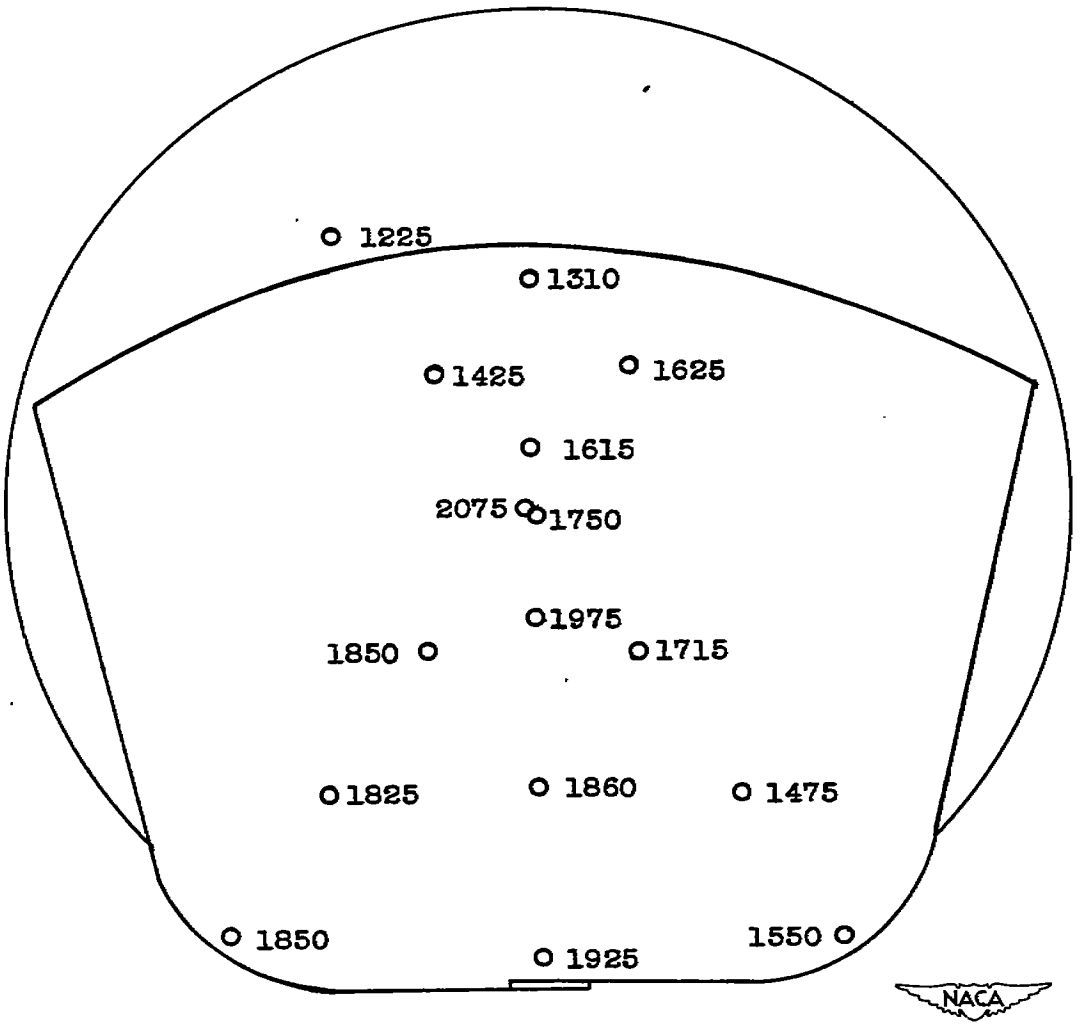

(b) Rotor speed, about 11,000 rpm.

Figure 13. - Continued. Temperature distribution in gas issuing from burner.

Security Classification of This Report Has Been Cancelled

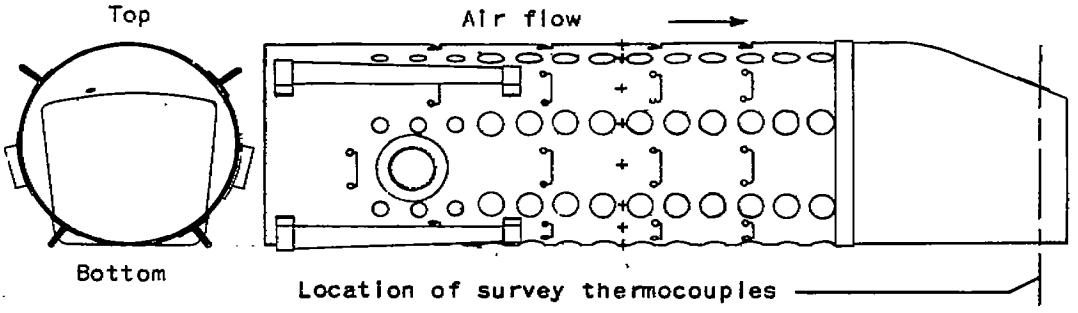

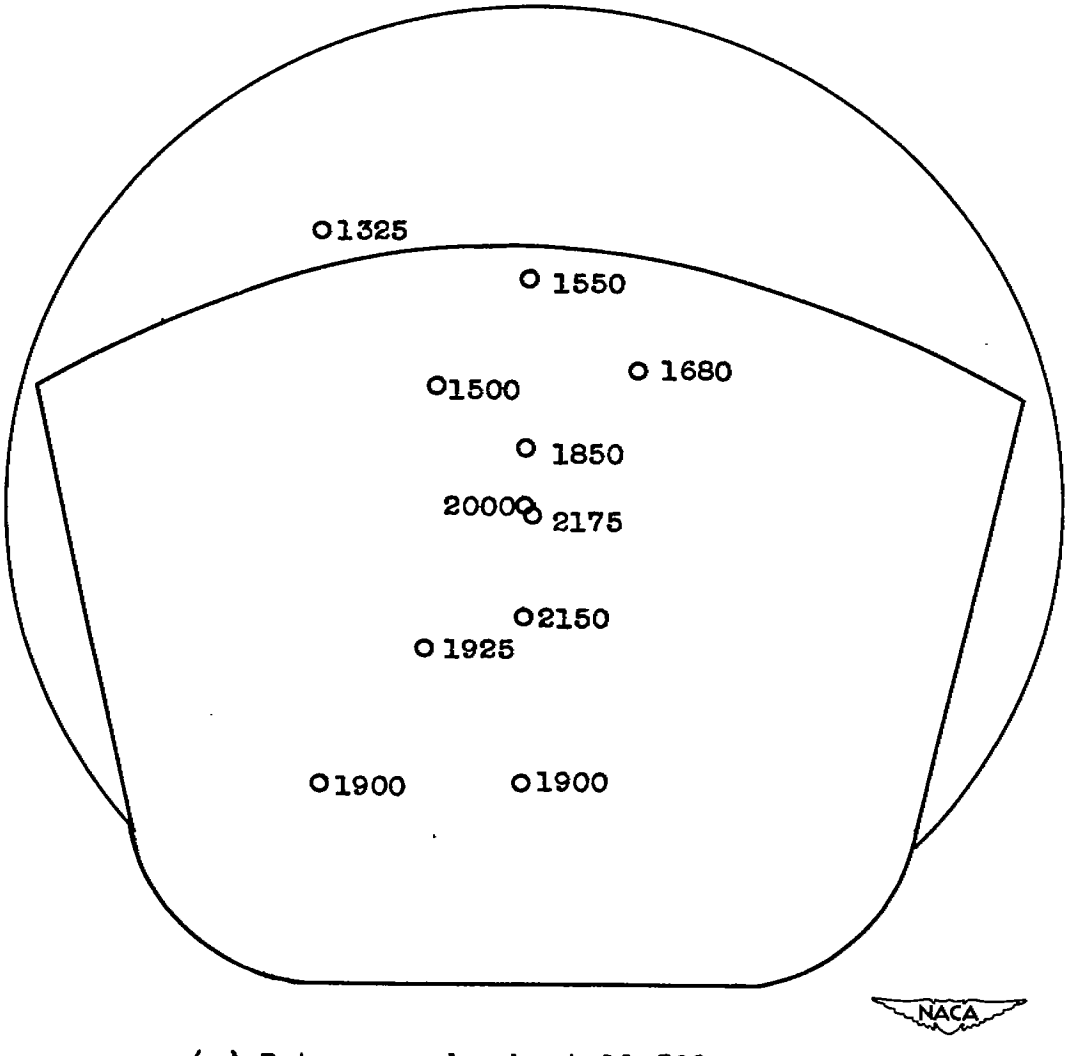

(c) Rotor speed, about 11,500 rpm.

Figure 13. - Concluded. Temperature distribution in gas issuing from burner.

698

Security Classification of This Report Has Been Cancelled

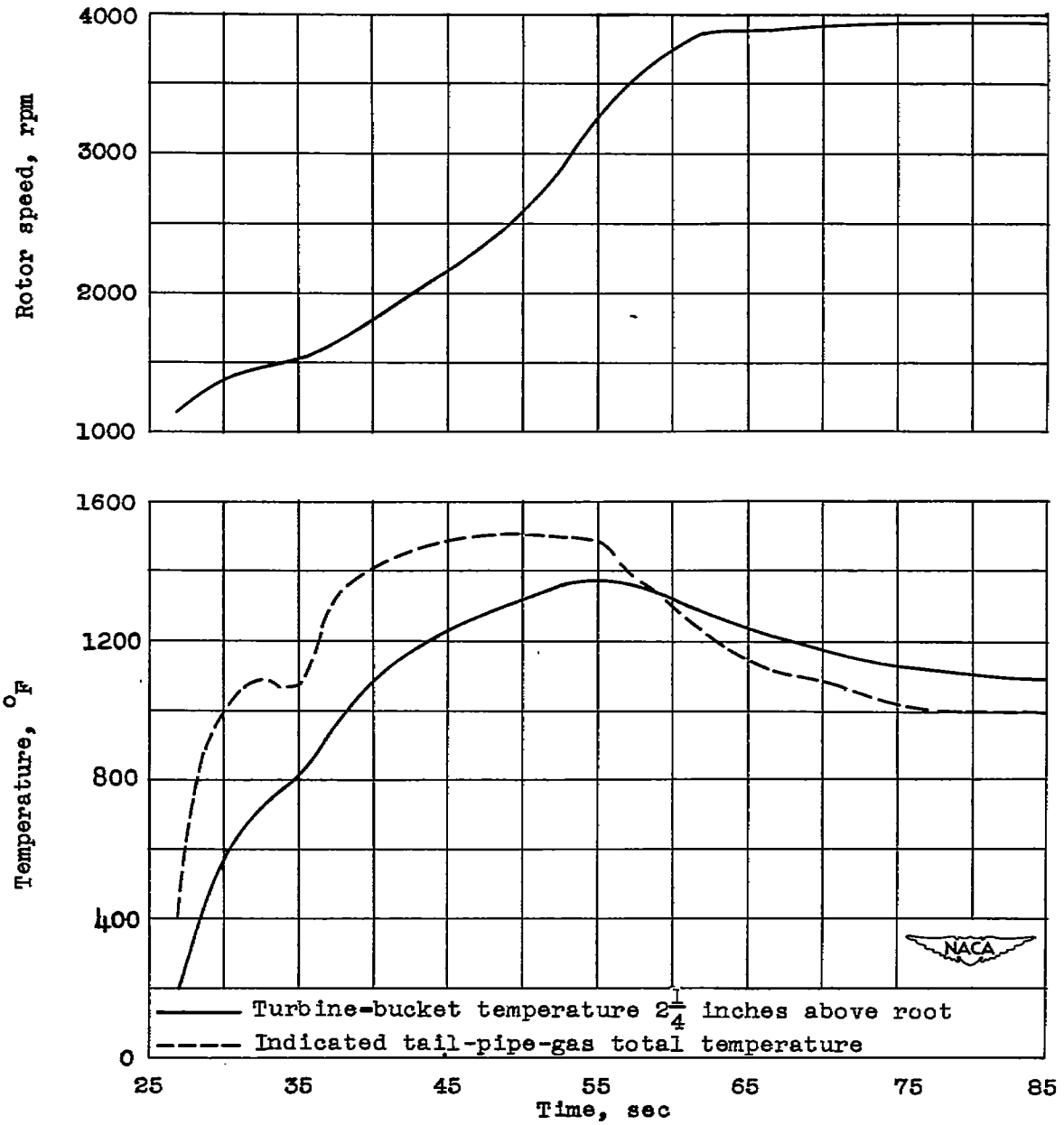

Figure 14. - Variation of rotor speed, turbine-bucket temperature, and tail-pipe-gas total temperature during starting interval of turbojet engine at beginning of run 2 (small tail-pipe nozzle).

Security Classification of This Report Has Been Cancelled

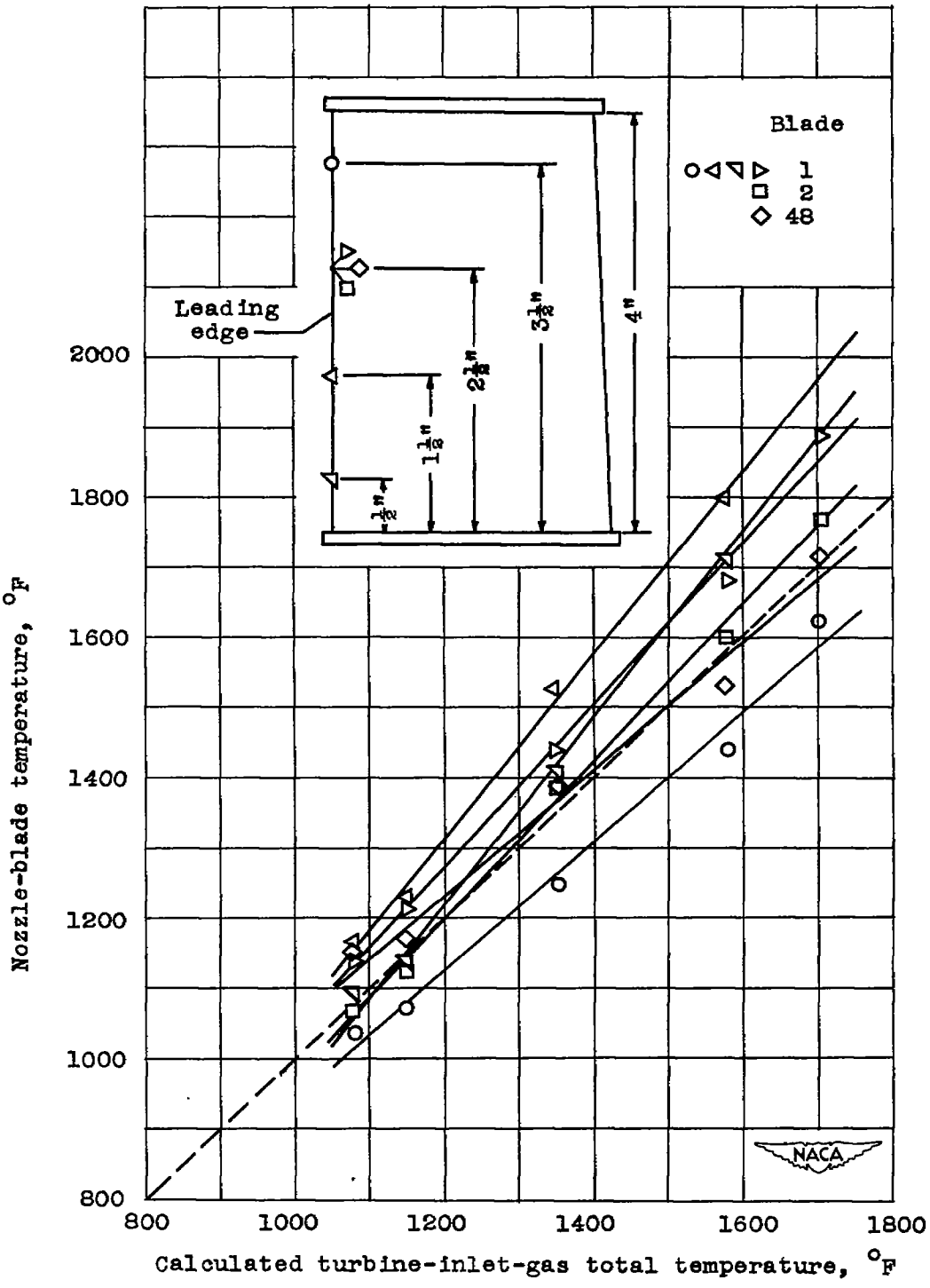

Figure 15. - Nozzle-blade temperature as function of calculated turbine-inlet-gas total temperature in turbojet engine for run 2 (small tail-pipe nozzle).

Security Classification of This Report Has Been Cancelled

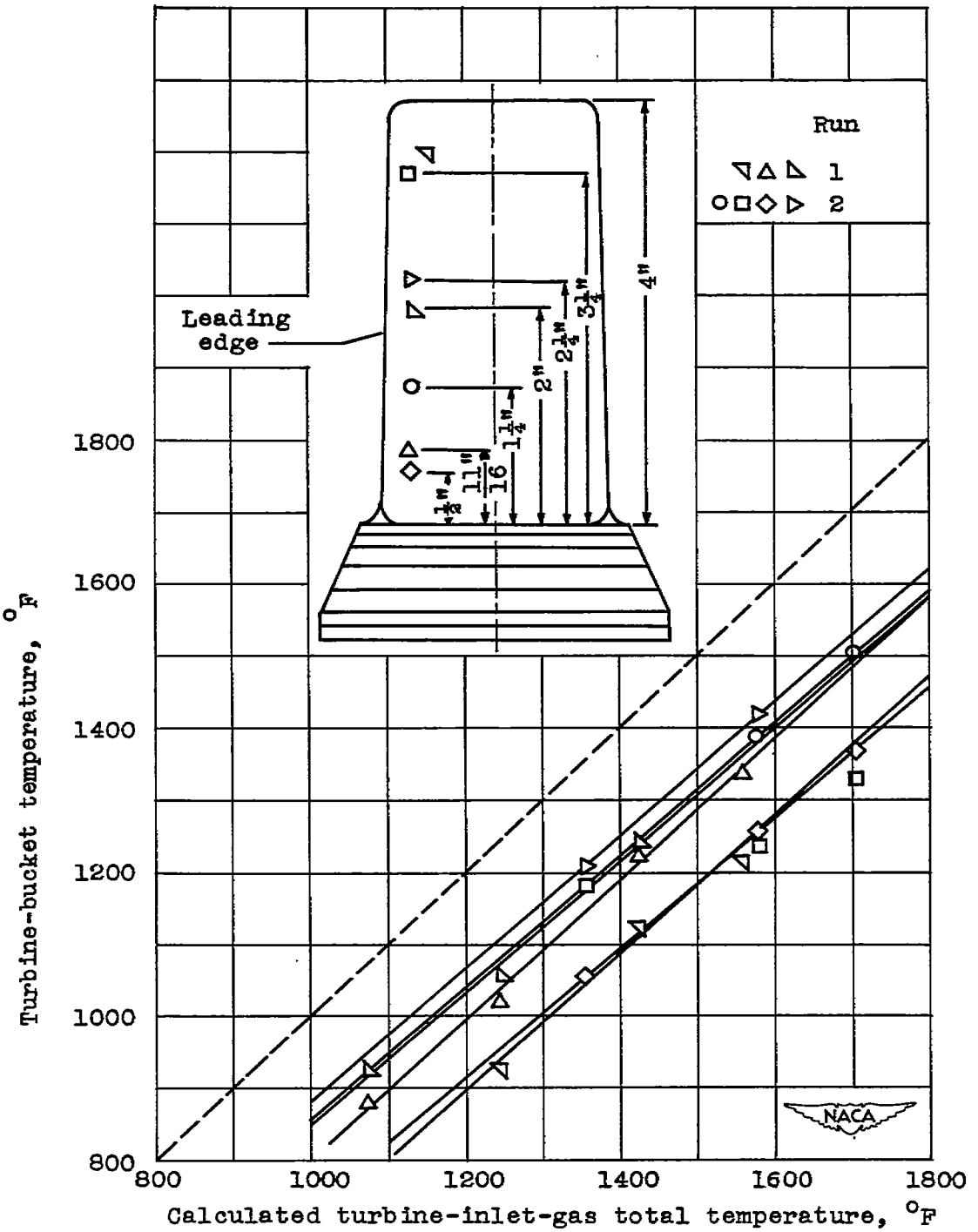

Figure 16. - Turbine-bucket temperature as function of calculated turbine-inlet-gas total temperature in turbojet engine for both runs.

Security Classification of This Report Has Been Cancelled